

## Different macroscopic models for slender and squat reinforced concrete walls subjected to cyclic loads

Jiuk Shin<sup>1a</sup> and JunHee Kim<sup>\*2</sup>

<sup>1</sup>*School of Civil and Environmental Engineering, Georgia Institute of Technology,  
790 Atlantic Drive, Atlanta, GA 30332-0355, USA*

<sup>2</sup>*Department of Architectural Engineering, Yonsei University,  
50 Yonsei-ro, Seodaemun-gu, Seoul 120-749, Republic of Korea*

*(Received March 27, 2014, Revised August 23, 2014, Accepted August 30, 2014)*

**Abstract.** The purpose of this study is to present adequate modeling solutions for squat and slender RC walls. ASCE41-13 (American Society of Civil Engineers) specifies that the aspect ratios of height to width for the RC walls affect the hysteresis response. Thus, this study performed non-linear analysis subjected to cyclic loading using two different macroscopic models: one of macroscopic models represents flexural failure of RC walls (Shear Wall Element model) and the other (General Wall Element model) reflects diagonal shear failure occurring in the web of RC walls. These analytical results were compared to previous experimental studies for a slender wall (> aspect ratio of 3.0) and a squat wall (= aspect ratio of 1.0). For the slender wall, the difference between the two macroscopic models was negligible, but the squat wall was significantly affected by parameters for shear behavior in the modeling method. For accurate performance evaluation of RC buildings with squat walls, it would be reasonable to use macroscopic models that give consideration to diagonal shear.

**Keywords:** macroscopic model; nonlinear analysis; reinforced concrete (RC) wall; aspect ratio

---

### 1. Introduction

Based on the results of existing experimental studies, ASCE41-13 (American Society of Civil Engineers, 2014) defines the behavior of reinforced concrete (RC) walls using the aspect ratio of height to width. According to their definition, slender walls with an aspect ratio exceeding 3.0 exhibit flexure-controlled behavior, while squat walls with an aspect ratio smaller than 1.5 displays shear-controlled behavior. The definition also states that RC walls with an aspect ratio falling in the range of 1.5-3.0 are under the influence of both flexural and shear behavior.

There is wide range of modeling methods from global models through component-based models to detailed models (Kim *et al.* 2010, 2012). Various models have been proposed for the analysis of RC walls. First, microscopic modeling methods derived from fundamental mechanics and theory can be considered in describing the accurate behavior of walls. Local behavior can be

---

\*Corresponding author, Assistant Professor, E-mail: [junhkim@yonsei.ac.kr](mailto:junhkim@yonsei.ac.kr)

<sup>a</sup>Ph.D. Student

examined using these methods, which usually employ finite element analysis (Gulec *et al.* 2009). However, the modeling process becomes complex if there are many finite elements to be considered, and more time is required for analysis (Kim *et al.* 2004; Tiong *et al.* 2013). On the other hand, macroscopic modeling methods are phenomena-based and focused on experimental results. They are thus more easily applicable than FEM to cases involving multi-story buildings or complex planes (Kim *et al.* 2004; Shin *et al.* 2014; Timothy 2010; Takabatake 2010). One limitation is that they are unable to accurately represent the shear behavior exhibited by webs of structural walls. To overcome the weakness of macroscopic analysis, several experiment-based macroscopic models have been developed.

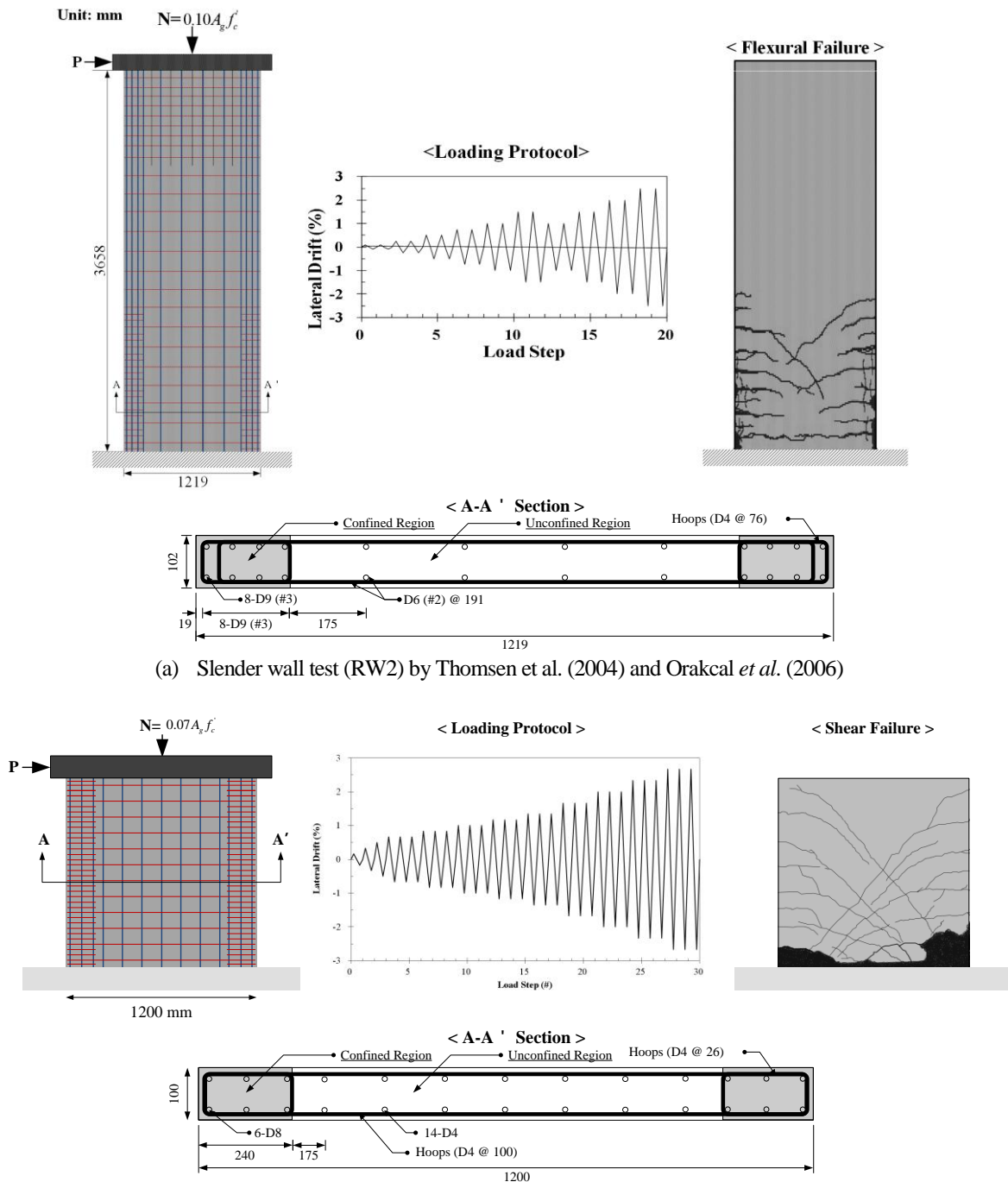
To represent flexural behavior, a 1984 study by Kabeyasawa *et al.* (1983) reflected shear behavior by placing two axial springs on both ends and applying a horizontal spring to the central rotational spring and the center of a member. Their study led to the development of the Multiple-Vertical-Line-Element Model (MVLEM) by Vulcano *et al.* (1998). This macroscopic model removed the central rotational spring and placed multiple axial springs to provide accurate descriptions of flexural behavior. Shear behavior was considered by installing a horizontal spring at the central area of the analysis model. Linde *et al.* (1993) simplified the MVLEM, representing flexural behavior through axial springs at both ends and the center, and reflecting shear behavior by installing horizontal and axial springs at the center. As shown in the experiments, the aforementioned macroscopic modeling methods are capable of providing comparatively accurate descriptions of flexural behavior, but have some limitations in reflecting the effect of shear behavior. This is because the behavior of squat walls with a small aspect ratio is significantly affected by diagonal shear cracks occurring in webs. Milve *et al.* (1996) developed a modified MVLEM, allowing more accurate descriptions of shear behavior. This model gave consideration to shear behavior using 2D panel elements, along with axial springs for flexural behavior. Recently, Park *et al.* (2007) presented a macroscopic model by applying the concept of strut-tie. Compared with existing experimental results, these macroscopic models offered more accurate predictions of the behavior of RC walls having a small aspect ratio because diagonal shear cracks were taken into account. From past studies, we can see that nonlinear diverse analysis models have been developed to provide accurate descriptions in accordance with aspect ratio.

The purpose of this study is to present adequate modeling solutions for RC walls with varying aspect ratios of height to width, and to develop guidelines for nonlinear structural analysis of shear wall structures. Cyclic testing results obtained from previous experimental studies (Thomsen *et al.* 2004; Orakcal *et al.* 2006; Salonikios *et al.* 1999, 2000) were analyzed for slender walls and squat walls with different aspect ratios as defined under ASCE41-13. The study proposed macroscopic modeling methods that give consideration to flexural behavior of the walls and shear behavior of webs in relation to the aspect ratio.

## 2. Experimental studies on structural walls

### 2.1 Background: shear behavior of structural walls

Flexural failure in RC walls appears as horizontal cracks at boundaries of RC walls (edges of RC walls, see dark gray regions of Fig. 5). Shear failure, on the other hand, can be classified into diagonal tension, diagonal compression, and sliding shear in the web of walls. Because of the increase of lateral displacement, diagonal tension produced wide diagonal cracks with yielding of transverse rebar. This failure mode is commonly seen in squat walls, in which there are less



(b) Squat wall test (LSW3) by Salonikios et al. (1999, 2000)

Fig. 1 Past experimental test programs and crack patterns

transverse reinforcements of webs. If transverse reinforcements are appropriately placed to prevent diagonal tension failure, diagonal compression failure may occur. Unlike diagonal tension failure, diagonal compression failure is more closely related to compression failure of concrete than yielding of reinforced bars. This diagonal failure tends to be brittle. Finally, sliding failure mode arises from compression failure of concrete in the lower section of walls when RC walls are subject to cycling loading (Gulec *et al.* 2009). For slender walls (aspect ratio exceeding 3.0), wide flexural cracks in the horizontal direction and small shear cracks in the diagonal direction are observed in the lower parts of webs. Shear cracks in slender walls have no significant effect on overall behavior. RC walls with the aspect ratio between 1.5 and 3.0 first exhibit cracks due to bending of boundary elements and followed by shear cracks in webs. Such walls display complex behavior associated with both flexural failure mode and shear failure mode.

## 2.2 Past experimental studies on slender walls and squat walls

Fig. 1 shows the front view and A-A' section, loading protocol, and failure mode of a slender wall (labeled as RW2) and squat wall (labeled as LSW3). Fig. 1(a) presents the experiment on slender walls conducted by Thomsen *et al.* (2004) and Orakcal *et al.* (2006), while 1(b) is that for squat walls performed by Salonikios *et al.* (1999, 2000). The RW2 specimen in Fig. 1(a) was designed based on ACI 318-08 (2008) and was tested at 1/4 the size of the actual wall. RW2 has an aspect ratio of 3.13 (3,658/1219 mm), and more than 25% of the total area is confined. The compressive strength and yielding strength of rebar are 27.4MPa and 414MPa respectively. Using the loading protocol shown in Fig. 1(a), lateral force and axial force ( $\cong$  340kN) were considered for the RW2 specimen. The axial force is 10% of wall axial load capacity based on nominal concrete strength and gross sectional area. At a lateral drift ratio of 0.75%, there was yielding of reinforcements in the confined region followed by flexural cracks. When the final lateral drift ratio of 2.5% was reached, flexural failure (horizontal cracks in the confined region) occurred as shown in Fig. 1(a). Meanwhile, LSW3 in Fig. 1(b) was designed based on EC8(1995) at 1/2.5 scale of the actual wall. LSW3 has an aspect ratio of 1.0 (thus classified as a squat wall), and its confined region amounts to 40% of the total area. Concrete and rebar were set as approximately 24MPa and 500MPa respectively. For the LSW3 specimen, a constant axial force ( $\cong$  210kN) and the loading protocol of Fig. 1(b) were considered. The axial force corresponds to 7% of the wall axial load capacity. The results show small flexural cracks in the lower section and then diagonal shear cracks in webs. The higher the lateral drift ratio, the more severe the shear cracks in webs. Such shear cracks led to smaller loads on RC walls. As presented in Fig. 1(b), the behavior of LSW3 is dominated by diagonal shear cracks. The two experiments demonstrate that flexural and shear mechanisms have different contributions to wall behavior depending on the aspect ratio, and that the walls undergo different flexural failure and shear failure modes. As such, in the design of structural walls, it is essential to apply an analysis model that gives consideration to behavioral characteristics. The next chapter proposes modeling methods in relation to the aspect ratio of walls.

## 3. Nonlinear modeling of RC wall

### 3.1 General Ideas of modeling

This study investigated the nonlinear behavior of RC walls using two macroscopic models for the purpose of practical application. The fiber-based analysis tool Perform3D(Computer and

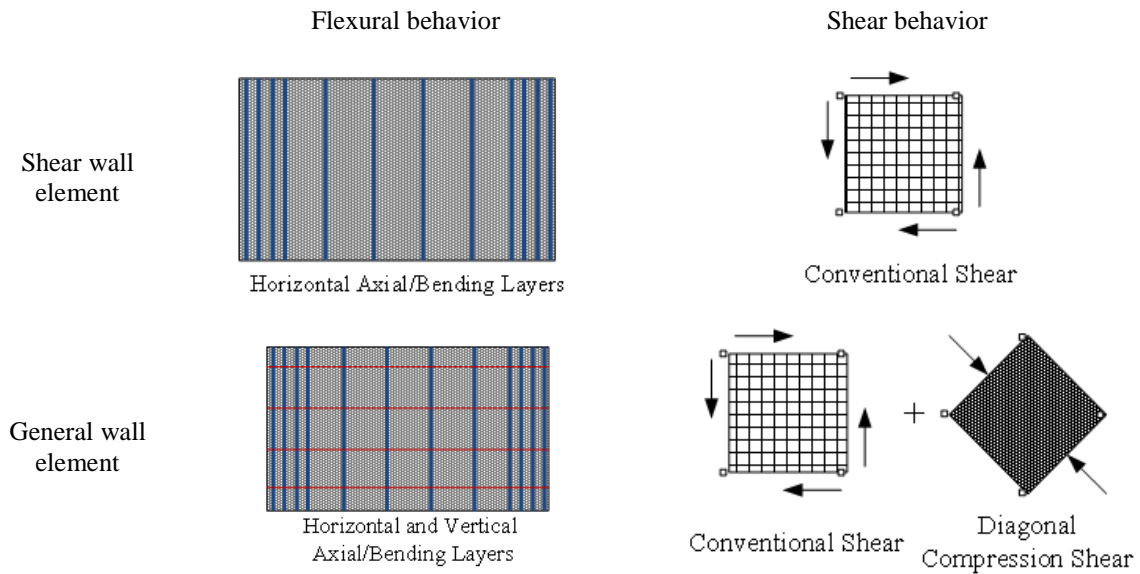


Fig. 2 Analytical element model for RC walls

Structures Inc. 2006) was used as it is more adequate for analysis at the structural system level and incurs less computational cost compared to FEM analysis. Since fiber-based analysis allows modeling based on inelastic fiber elements, it is able to provide accurate descriptions of complex behavior exhibited by rebar and concrete. Fig. 2 shows the macroscopic modeling methods considered in this study and the applicable elements. Similar to the previously developed MVLEM (Vulcano *et al.* 1987), the Shear Wall Element of Fig. 2 takes into account longitudinal reinforcements and conventional shear. The shear behavior exhibited when walls are subject to loading in the transverse direction has been defined as conventional shear. The General Wall Element method presented in Fig. 2 provides more detailed modeling as it considers a greater number of factors than the Shear Wall Element modeling method. This modeling method represents flexural behavior by placing horizontal/vertical reinforcements and considering conventional shear and diagonal compression shear at the same time. Here, diagonal compression shear refers to behavior resisting to concrete compression failure in the diagonal direction in the webs of RC walls (CEN 1995). The General Wall Element method in Fig. 2 is similar to LDLEM (Linde *et al.* 1993), developed to reflect shear behavior, the modified MVLEM (Milev *et al.* 1996), and the strut-tie model (Park *et al.* 2007). Difference between Shear Wall Element and General Wall Element is associated with the directions of applied rebar and the consideration of shear behavior. To review the adequacy of the two macroscopic modeling methods (Shear Wall Element and General Wall Element), nonlinear analysis was performed for the two walls mentioned in Section 2.2, and comparisons were made with experimental results.

### 3.2 Material modeling

Fig. 3 shows the hysteresis behavior of concrete and rebar. Fig. 3(a) gives the concrete material model for the Y-U-L-R-X range. This can be used to describe in detail the hysteresis

characteristics of nonlinear concrete material. The range of each strain is explained below.

- Y-Point: Considers yield strain and stress.
- Range of Y-U: Considers strain hardening ratio of material.
- Range of U-L: Represents strain and stress for ductile limit with a strain hardening ratio of 0 (U and L are extreme points of stress and strain).
- Range of L-R: Represents decrease in stress of material used (R-point is the remaining stress of material).
- Range of X: Maximum strain of material that can be reflected in computational analysis.

Material characteristics of rebar in 3(b) are more simplified than that of concrete in Fig. 3(a) and exhibited over the Y-U-X range. The L-R for material softening was omitted. The description of each range is the same as that for concrete.

The cross-sections (See Fig. 1 and Fig. 5: dark gray – confined regions and light gray – unconfined regions) in the horizontal direction for specimens used in this study were comprised of unconfined regions and confined regions. The characteristics of each region were considered

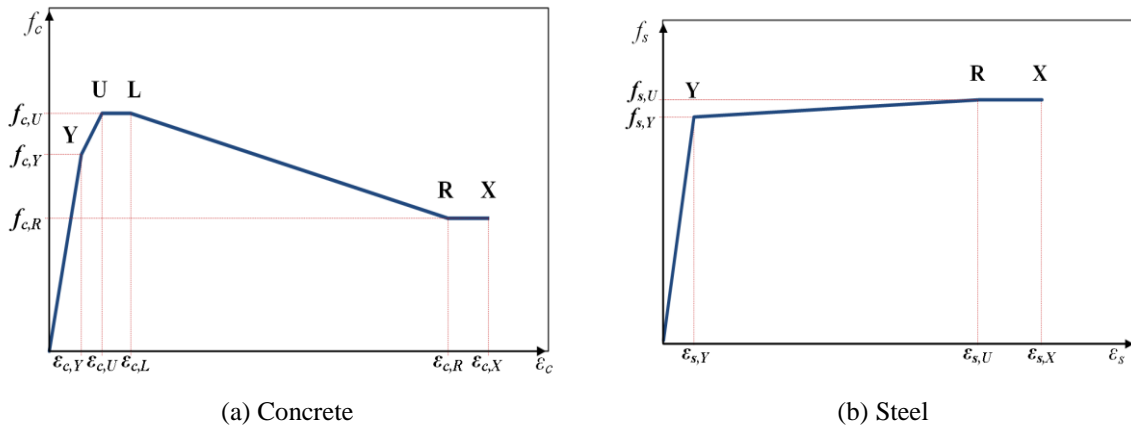


Fig. 3 Nonlinear models for concrete and steel materials

Table 1 Material properties of concrete and rebar

| Point | RW2 (Slender wall) |             |              |             |                 |             |              |             | LSW3 (Squat wall) |             |              |             |                 |             |              |             |
|-------|--------------------|-------------|--------------|-------------|-----------------|-------------|--------------|-------------|-------------------|-------------|--------------|-------------|-----------------|-------------|--------------|-------------|
|       | Unconfined region  |             |              |             | Confined region |             |              |             | Unconfined region |             |              |             | Confined region |             |              |             |
|       | Concrete           |             | Rebar        |             | Concrete        |             | Rebar        |             | Concrete          |             | Rebar        |             | Concrete        |             | Rebar        |             |
|       | $\epsilon_c$       | $f_c$ (MPa) | $\epsilon_s$ | $f_s$ (MPa) | $\epsilon_c$    | $f_c$ (MPa) | $\epsilon_s$ | $f_s$ (MPa) | $\epsilon_c$      | $f_c$ (MPa) | $\epsilon_s$ | $f_s$ (MPa) | $\epsilon_c$    | $f_c$ (MPa) | $\epsilon_s$ | $f_s$ (MPa) |
| Y     | 0.0017             | 39.92       | 0.0021       | 448         | 0.0018          | 40.25       | 0.0022       | 414         | 0.0025            | 17.90       | 0.0031       | 610         | 0.0043          | 29.38       | 0.0029       | 585         |
| U     | 0.0018             | 43.45       | -            | -           | 0.0025          | 47.65       | -            | -           | 0.003             | 19.89       | -            | -           | 0.0052          | 32.65       | -            | -           |
| L     | 0.002              | 43.45       | -            | -           | 0.004           | 47.65       | -            | -           | 0.0034            | 19.89       | -            | -           | 0.0057          | 32.65       | -            | -           |
| R     | 0.0135             | 0.43        | 0.02         | 460         | 0.015           | 32.97       | 0.02         | 426         | 0.0087            | 0.20        | 0.05         | 640         | 0.04            | 10.65       | 0.05         | 615         |
| X     | 0.02               | 0.43        | 0.03         | 460         | 0.02            | 32.97       | 0.03         | 426         | 0.05              | 0.20        | 0.06         | 640         | 0.05            | 10.65       | 0.06         | 615         |

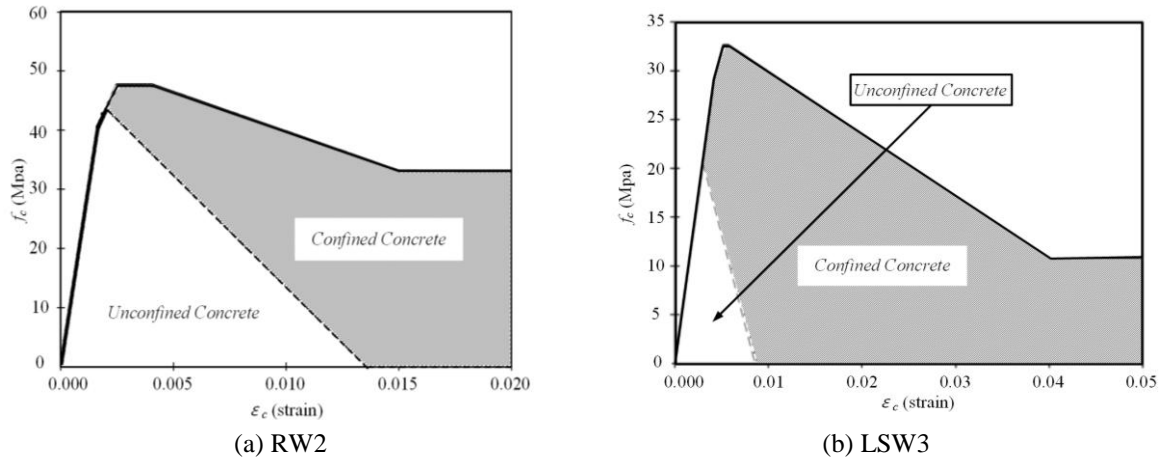


Fig. 4 Stress-strain relationship for confined and unconfined concrete of RW2

through different placements of reinforcements during computer modeling and application of material properties. Past studies on the stress-strain relationship of concrete show a significant increase in strength and ductility in the confined region, which is surrounded by stirrups. However, concrete in the unconfined region undergoes brittle failure after hitting ultimate strength. Table 12 shows the strain and stress for D9 in the confined region, D6 in the unconfined region of RW2. D8 and D4 correspond to the confined region and unconfined region of LSW3, respectively. To obtain more accurate results, we considered the actual experimental results instead of the design strength of rebar and concrete. The stress-strain relationship of concrete in Table 1 was calculated using the model presented by Mander *et al.* (1988). The results are shown in detail in Table 1, with consideration of the stress-strain curves presented in Fig. 3. In the concrete material, the tensile behavior was neglected. For the rebar used in walls, Y-U-X points were decided (Table 1) after comparing experimental results of existing studies (Thomsen *et al.* 2004; Salonikios *et al.* 1999, 2000) and the hysteresis characteristics of rebar in Fig. 3(b), and equal consideration was given to tensile and compression. Fig. 4 displays the concrete strain-stress characteristics for Y-U-L-R-X values of confined (solid line) and unconfined concrete (dotted line) of RW2 and LSW3, as given in Table 1.

### 3.3 Macro modeling of RC walls

Fig. 5 shows the analysis model resulting from application of the two methods (Shear Wall Element model and General Wall Element model) to the specimens considered in this study. The horizontal cross-sections of RW2 and LSW3 specimens were modeled into confined (color: dark gray) and unconfined (color: light gray) regions using inelastic fiber elements. The area of rebars/area of concrete can be seen from the horizontal rebars in confined and unconfined regions, as shown in Fig. 5(a) and 5(b). While the Shear Wall Element model only considered the horizontal rebars, the General Wall Element model added the vertical rebars. Furthermore, the Shear Wall Element only takes into account conventional shear, but the General Wall Element model considers both diagonal compression shear and conventional shear in webs (unconfined region). The shear models considered in this study are assumed to exhibit bilinear behavior. The

yield shear strength for conventional shear was calculated by dividing yield moment strength over wall height, and diagonal compression shear was subject to the effective compression strength equation of strut presented in ACI 318-08. Fig. 6 gives the stress-strain relationship of diagonal compression shear ( $\beta$  is equal to 0.6.).

To reflect the reduction in stiffness in hysteresis behavior of walls from cyclic loading, the stiffness reduction factor was applied to reinforcements. This is because energy dissipation is governed by reinforcements due to the brittle characteristic of concrete materials (Eom *et al.* 2004; Kim *et al.*, 2009). Using the Energy Dissipation Factor (EDF), stiffness reduction was applied to each range (Y-U-X). Fig. 7 shows the hysteresis behavior before (dotted line) and after (solid line) applying EDF. EDF is the area of the degraded hysteresis region (A) divided by the non-degraded hysteresis region (B). This factor will become smaller in accordance with increasing displacement.

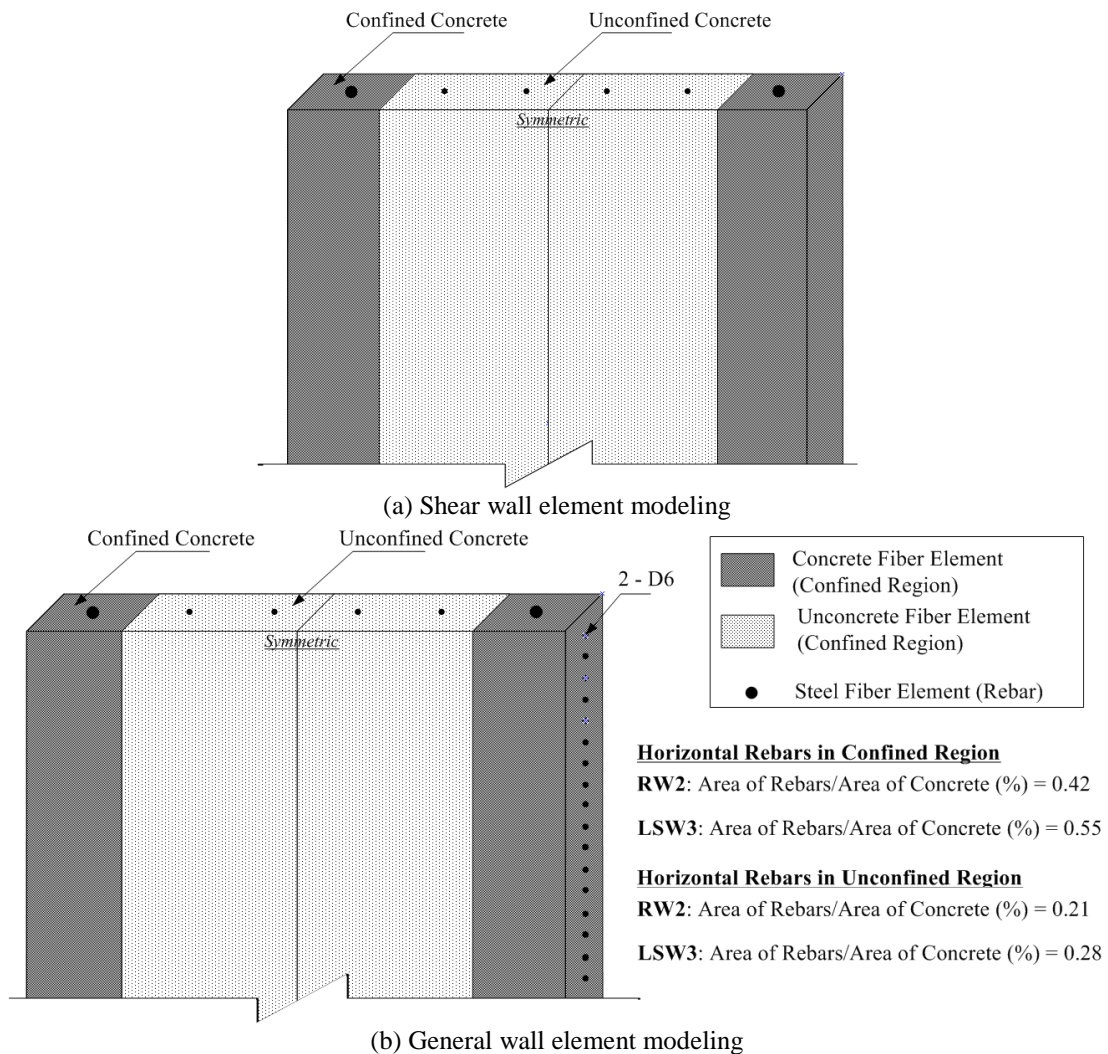


Fig. 5 Computational modeling for concrete walls RW2 & LSW3

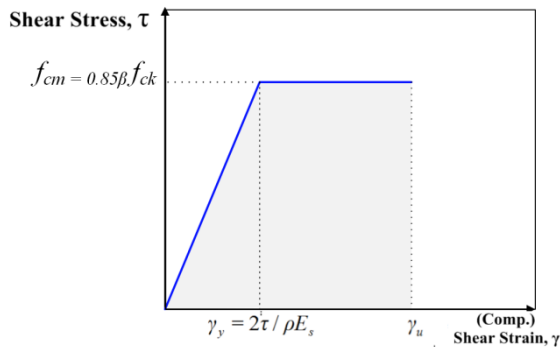


Fig. 6 Shear stress-strain relationship

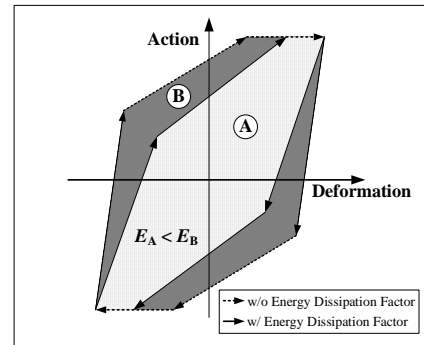


Fig. 7 Hysteretic loops with and without EDF

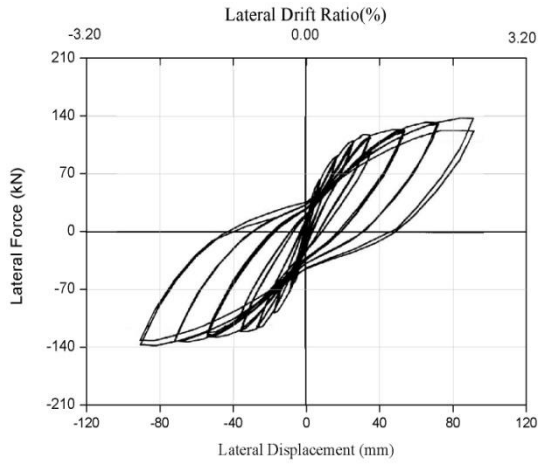
This study applied EDF to each range of the hysteresis model based on experimental results through trial-and-error. This is because it is difficult to consider every stiffness change subjected to cyclic loading in all three ranges (Y-U-X) or four ranges (Y-U-R-X) of the hysteresis model. The results of nonlinear analysis, based on the analytical modeling process described in this section, are given in the following section.

#### 4. Results of nonlinear analysis

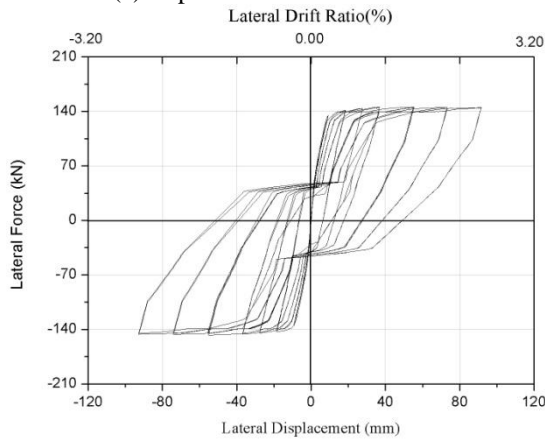
This section presents the nonlinear analysis results for two RC walls (RW2 and LSW3) with different aspect ratios. To make comparisons between macroscopic modeling methods introduced in the previous chapter and hysteresis behavior (load-displacement curves) of RC walls in past experimental studies, the same loading protocols (Fig. 2) were applied to the computational simulation. Based on the displacement-load hysteresis curves derived from nonlinear analysis, energy dissipation areas were calculated to compare lateral resistance capacity of RC walls by modeling method.

##### 4.1 Hysteretic load– displacement curves

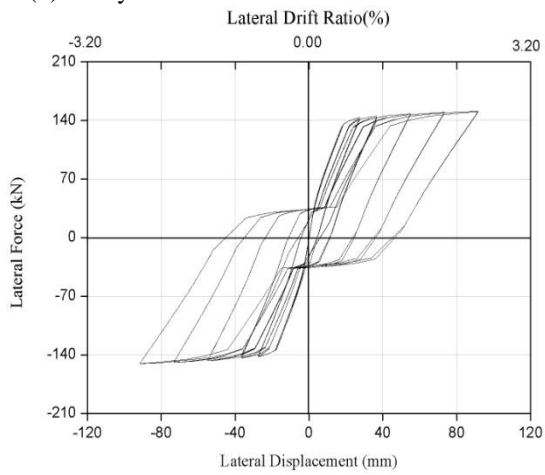
Fig. 8 presents the analysis results for load-displacement of the RW2 model based on the Shear Wall Element method (Fig. 8 (b)) and the General Wall Element method (Fig. 8 (c)) along with test results (a) to allow comparison. When the maximum value of each cycle was compared, the analysis models based on the General Wall Element method and Shear Wall Element method had a difference of 22% and 24%, respectively, for 0.5% interstory drift ratio. In other cycles, the difference between analysis and test results for the General Wall Element method was smaller than 9%. However, in cycles other than that having 0.5% interstory drift ratio, the Shear Wall Element method resulted in 16% or less difference between analysis and test results. Although the General Wall Element method gave slightly more accurate results than the Shear Wall Element model in general for the RW2 analysis model, modeling methods did not lead significant differences in results. As demonstrated in RW2 experiments, shear behavior has minimal effect on the overall behavior of slender walls as they are dominated by flexural behavior.



(a) Experimental test result

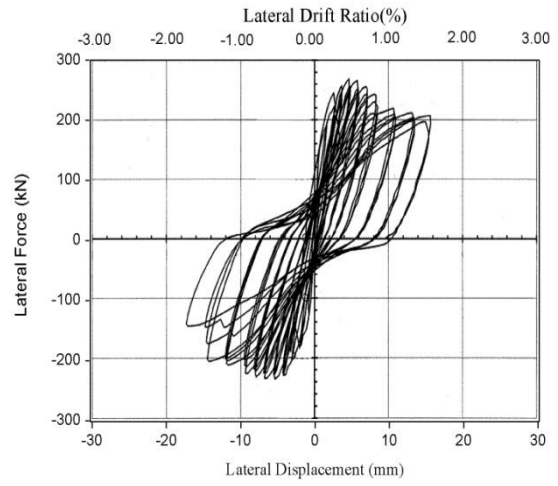


(b) Analysis result with shear wall element

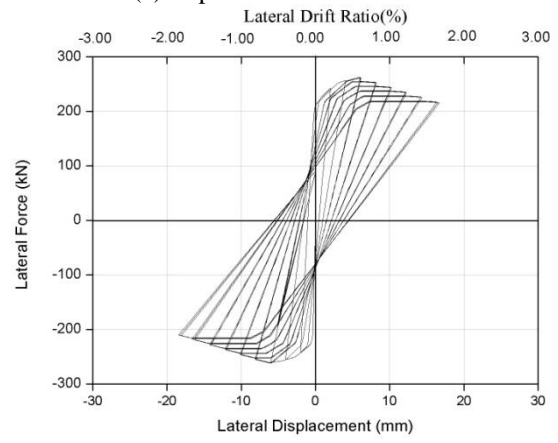


(c) Analysis result with general wall element

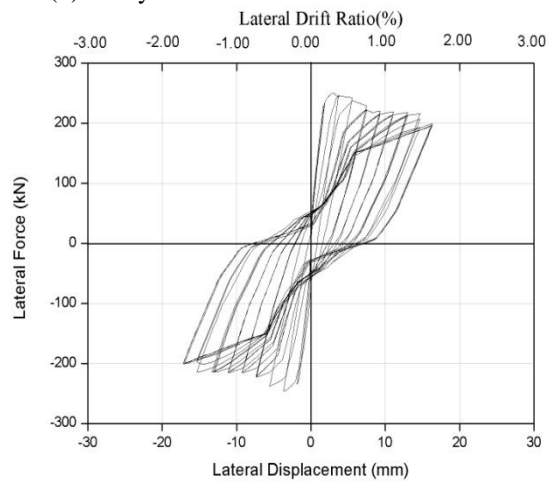
Fig. 8 Hysteretic load-displacement curves for RW2



(a) Experimental test result



(b) Analysis result with shear wall element



(c) Analysis result with general wall element

Fig. 9 Hysteretic load-displacement curves for LSW3

Fig. 9 gives the load-displacement hysteresis curves of LSW3 based on the Shear Wall Element (Fig. 9 (b)) method and General Wall Element (Fig. 9 (c)) method, along with test results (Fig. 9 (a)) by Salonikios *et al.* (1999, 2000). From the nonlinear analysis results presented in Fig. 9(a), some degradation in strength and stiffness is observed with cyclic loading, but the pinching effect arising from shear behavior of concrete walls is not accurately predicted. As can be seen in Fig. 9, the LSW3 analysis model based on the General Wall Element method provides more accurate results for hysteresis behavior with cyclic loading compared to the Shear Wall Element method. When maximum lateral forces are compared for each cycle, the LSW3 model based on the Shear Wall Element method gives 30% to 50% difference between test results and analysis results for the first, second, and final cycle. The results were fairly consistent for the other cycles. As for the LSW3 model based on the General Wall Element method, maximum values for lateral forces only had a small difference of 10% or less when compared to test results. To summarize for the LSW3 analysis model, lateral forces differed by up to 40% depending on modeling method. The analysis model based on the General Wall Element method was found to produce behavior similar to actual test results for squat walls like LSW3. This is because the General Wall Element model takes into account diagonal compression shear, which reflects diagonal shear cracks in the webs of squat walls, unlike the Shear Wall Element model that only considers Conventional Shear.

#### 4.2 Cumulative energy dissipation

This section estimates cumulative energy dissipation based on the load-displacement hysteresis curves shown in Fig. 8 and Fig. 9. The cumulative energy dissipation is a useful measurement of seismic efficiency for structural members. This is to show differences of the lateral resisting capacities of the RC walls between experimental and analytical results obtained from different modeling methods. Hysteresis energy dissipation is represented by the area of load-displacement hysteresis curves for each loading cycle. Cumulative energy dissipation was then derived from summing the hysteresis energy dissipation of each cycle for the considered loading protocols.

Fig. 10 shows the cumulative energy dissipation of RW2 (Fig. 10(a)) and LSW3 (Fig. 10(b)) for the Shear Wall Element method and General Wall Element method. The figure also shows total cumulative energy dissipation from test results for comparison. As shown in Fig. 10(a), the RW2 analysis model has a small difference of 5% between the Shear Wall Element and General Wall Element during the 20th cycle, which corresponds to the final loading protocol. In the actual experiment, the cumulative energy dissipation of RW2 had a difference of 9-14%. In the case of LSW3 shown in Fig. 10(b), the model based on the General Wall Element method was approximately 76% (44.45kN-m/25.32kN-m) greater than that of the Shear Wall Element method at the 18th loading protocol. When compared with actual test results, the General Wall Element model had a small difference of 5% (46.2kN-m/44.45kN-m), whereas the Shear Wall Element model differed by more than 80% (46.2kN-m/25.32kN-m). As for cumulative energy dissipation by modeling method, the difference was negligible in slender walls (RW2), but underestimated results were obtained from the Shear Wall Element method for squat walls (LSW3) compared to the General Wall Element method. In particular, differences arising from the choice of modeling method become greater for LSW3 with increasing lateral drift ratio. This implies that modeling methods will have a significant impact on evaluating the seismic performance of buildings when structural analysis is performed for shear wall structures.

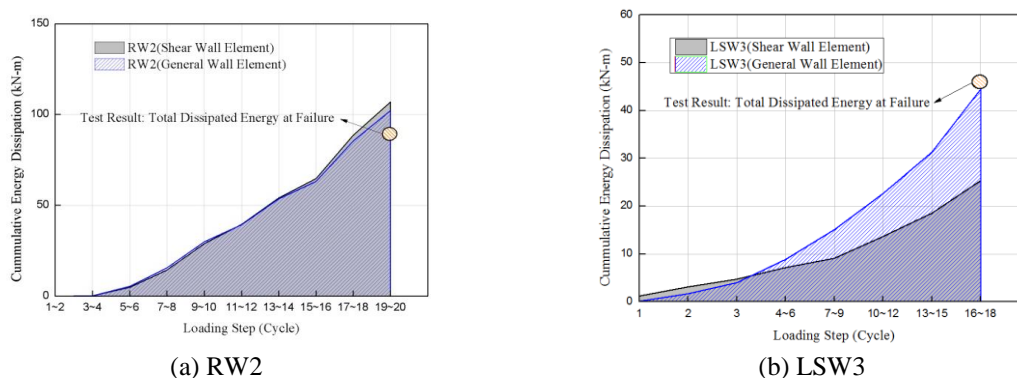


Fig. 10 Cumulative energy dissipation

## 5. Conclusion

This study conducted nonlinear analysis of RC walls with different aspect ratios of width to height using two macroscopic models, and compared the results with existing experimental studies. An appropriate analysis model with consideration of the aspect ratio was proposed for buildings that include structural walls.

1) For the squat wall (LSW3), maximum displacement and strength for each loading step showed slight difference depending on the macroscopic modeling methods (Shear Wall Element and General Wall Element methods). However, by the modeling methods, the cumulative energy dissipations indicated significant difference. When comparing the analytical results with the past test result (Salonikios *et al.* 1999, 2000), the Shear Wall Element modeling overestimated approximately 80% of the cumulative energy dissipation for the test results. However, the General Wall Element modeling estimated the similar cumulative energy dissipation with the test result. The reason for those evaluations is that the General Wall Element modeling enables to consider the diagonal compression shear, which occurs in web of the squat wall.

2) Through nonlinear analysis, two different modeling methods considered in this study estimate accurate lateral resisting capacity for the slender wall, governed by flexural wall. This estimation indicates that flexural behavior of the walls can be predicted regardless of the modeling methods. However, parameters of the modeling methods significantly affect the squat wall's resisting capacity. From this observation, it is concluded that the squat wall will be estimated by the macroscopic models, which enable to predict shear behavior of the real wall. As similar modeling methods with the general wall modeling, modified MVLEM developed by Milve *et al.* (1996), and LDLEM developed by Park *et al.* (2007) will be considerable. Through this study, for accurate seismic performance evaluation of buildings with structure walls, it would be reasonable to employ appropriate modeling methods depending on aspect ratio of the walls.

## Acknowledgments

The research described in this paper was financially supported in part by 2013 Yonsei University Research Fund.

## References

- ACI Building Code Requirements for Structural Concrete and Commentary (2008), ACI 318-08, American Concrete Institute, Detroit, Mich.
- AIK-Architectural Institute of Korea (2009), Korea Building Code - KBC 2009.
- ASCE (2014), Seismic Evaluation and Retrofit of Existing Buildings, ASCE/SEI 41-13, American Society of Civil Engineers.
- CEN Technical Committee 250/SC8 (1995), "Eurocode 8: Earthquake Resistant Design of Structures – Part 1: General Rules (ENV 1998 1-1, 1-2 and 1-3)", CEN, Brussels.
- Computer and Structures Inc. (2006), Nonlinear Analysis and Performance Assessment for 3D Structures, Berkeley, CA.
- Eom, T.S. and Park, H.G. (2004), "Energy-based hysteretic models for R/C members", *J. Earthq. Eng. Society Korea*, **8**(5), 45-54.
- Gulec, C.K. and Whittaker, A.S. (2009), *Performance-Based Assessment and Design of Squat Reinforced Concrete Shear Walls*, Technical Report No. MCEER-09-0010, MCEER, University at Buffalo, State University of New York.
- Kabeyasawa, T., Otani, S. and Aoyama, H. (1983), "Nonlinear earthquake response analysis of RC wall frame structure", *Trans. Japan Conc. Institute*.
- Kim, J.H., Ghaboussi J. and Elnashai A.S. (2010), "Mechanical and informational modeling of steel beam-to-column connections", *Eng. Struct.* **32**(2), 449-458.
- Kim, J.H., Ghaboussi J. and Elnashai A.S. (2012), "Hysteretic mechanical–informational modeling of bolted steel frame connections", *Eng. Struct.* **45**, 1-11.
- Kim, T.W., Foutch, D.A., LaFave, J.M. and Wilcoski, J. (2004), "Performance assessment of reinforced concrete structural walls for seismic loads", Structural Research Series - No. 634, Dept. of Civil and Environmental Engineering, University of Illinois at Urbana-Champaign.
- Kim, M.S., Yun S.H., Lee Y.H. and Kim H.C. (2009), "Analysis of lateral retrofitting effect by FRP and BRB for beam-column element joint of low-rise piloti buildings", *J. Earthq. Eng. Society Korea*, **13**(2), 69-77.
- Linde, P. (1993), *Numerical Modeling and Capacity Design of Earthquake-Resistant Reinforced Concrete Walls*, Report No. 200, Institute of Structural Engineering, Swiss Federal Institute of Technology (ETH), Zurich, Birkhauser, Basel.
- Mander, J.B., Priestley, M.J.N. and Park, R. (1988), "Theoretical stress-strain model for confined concrete", *J. Struct. Eng. ASCE*, **114**(8), 1804-1826.
- Milev, J. (1996), "Two-dimensional analytical model of reinforced concrete shear walls", *Proceeding of 11th World Conference Earthquake Engineering*, Paper No. 320.
- Orakcal, K., Massone, L.M. and Wallace, W.J. (2006), "Analytical modeling of reinforced concrete walls for predicting flexural and coupled-shear-flexural response", Pacific Earthquake Engineering Research Center, University of California, Los Angeles.
- Park, H.G. and Eom, T.S. (2007), "Truss model for nonlinear analysis of RC members subjected to cyclic loading", *J. Struct. Eng.*, **133**(10), 1351-1363.
- Salonikios, T.N., Kappos, A.J., Tegos, I.A. and Penelis, G.G. (1999), "Cyclic load behavior of low-slenderness reinforced concrete walls: design basis and test results", *ACI Struct. J.*, **96**(4), 649-660.
- Salonikios, T.N., Kappos, A.J., Tegos, I.A. and Penelis, G.G. (2000), "Cyclic load behavior of low-slenderness reinforced concrete walls: Failure modes, strength analysis, and design implications", *ACI Struct. J.*, **97**(1), 132-141.
- Shin, J., Kim, J. and Lee, K. (2014), "Seismic assessment of damaged piloti-type RC building subjected to successive earthquakes", *Earthq. Eng. Struct. D.*: doi: 10.1002/eqe.2412.
- Sullivan, T.J. (2010), "Capacity design considerations for RC frame-wall structures", *Earthq. Struct.*, **1**(4), 391-410.
- Takabatake, H. (2010), "Two-dimensional rod theory for approximate analysis of building structures",

- Earthq. Struct.*, **1**(1), 1-19.
- Thomsen, J.H. and Wallace, J.W. (2004), "Displacement-based design of slender reinforced concrete structural walls - experimental verification", *J. Struct. Eng.*, ASCE, **130**(4), 618-630.
- Tiong, P.L.Y., Adnan, A. and Hamid, N.H.A. (2013), "Behaviour factor and displacement estimation of low-ductility precast wall system under seismic actions", *Earthq. Struct.*, **5**(6), 625-655.
- Vulcano, A. and Bertero, V.V. (1987), *Analytical Models for Predicting the Lateral Response of RC Shear Walls: Evaluation of Their Reliability*, Report No. UCB/EERC-87/19, EERC, University of California, Berkeley, California.